LASER
& PHOTONICS
REVIEWS

Laser Photonics Rev. **8,** No. 3, 394–408 (2014) / **DOI** 10.1002/lpor.201300168

REVIEW
ARTICLE

Abstract Plasmonics has attracted a lot of interest in the past few years because of its unique features, especially for its ability to confine light in extremely small volumes. However, application of plasmonics is restricted by the large propagation loss associated with plasmonic waveguides. On the other hand, dielectric waveguides enjoy low loss, although the mode confinement is relatively weaker. Hybrid plasmonic waveguides (HPWGs), which combine these two guiding mechanisms, allow one to utilize the benefits of both technologies. Over the past few years there have been intense research activities around the world on this new guiding scheme. In this work the operating principle of HPWGs, various HPWG structures proposed by different research groups, and their potentail applications are reviewed.

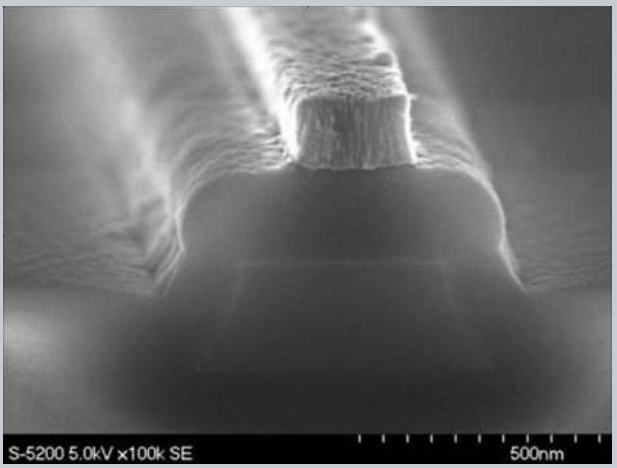

A marriage of convenience: Hybridization of surface plasmon and dielectric waveguide modes

Muhammad Z. Alam *, J. Stewart Aitchison, and Mo Mojahedi

1. Introduction

Recent progress in nanofabrication has given researchers the ability to control the structure and properties of materials at an unprecedented level. A combination of this progress and the availability of high performance computing resources have revolutionized many branches of science and technology, notable among them photonics. One very promising branch of photonics is plasmonics which deals with the study and application of surface plasmons (SPs) [1–3]. SPs are surface waves supported by metal-dielectric interfaces at optical wavelengths. SPs have many attractive features for example, high field intensity at the metal-dielectric interface, resonant behavior, ability to confine light at nanometer scales, and slow group velocity. These features make plasmonics attractive for many applications ranging from integrated optics, biosensing, solar cells, nanolithography and near field microscopy. At optical wavelengths metals have complex permittivity, and as a result plasmonics waveguides suffer from large propagation losses, which poses a challenge. Plasmonic waveguides losses are proportional to their optical mode confinement, i.e. more confined modes suffer more losses. To achieve a satisfactory compromise between the loss and confinement many different plasmonic guides have been proposed including the metal slot [4–6], the insulator-metal-insulator [7], channel [8], the dielectric loaded metal [9], and metal wedge [10]; but the large propagation losses still limit the usefulness of plasmonic waveguides for many applications.

A comparison of standard dielectric waveguide with a plasmonic waveguide reveals that the advantages and limitations of these guides are complimentary. This is illustrated by comparing the guided power density profiles of a silicon-on-insulator (SOI) waveguide and a metal slot plasmonic waveguides which are shown in Fig. 1(a) and (b). The SOI waveguide provides the highest level of confinement among all dielectric waveguides, and the loss of such a guide can be very low (less than 1 dB/cm), but as shown in Fig. 1(c) the mode size for such a waveguide is still several hundred nanometers. In contrast, as shown in Fig. 1(d), the mode size of a plasmonic slot waveguide can be less than 50 nm but the propagation loss is more than 5000 dB/cm.

A natural question to ask is what happens if we try to combine these two guiding mechanisms? The answer is the hybrid plasmonic waveguide (HPWG) which is a new branch of plasmonics that has been receiving a growing amount of interest. Although the field of hybrid plasmonics is only few years old, the activities in this area have been impressive. A large number of papers have been published which have proposed various types of HPWG structures, have examined their guiding principle and modal characteristics, and have considered applications of HPWG ranging from polarizers, ring resonators, couplers, nonlinear optics, biosensors, and nanolasers. This review paper aims at

Department of Electrical and Computer Engineering, University of Toronto, Toronto M5S3G4, Canada
*Corresponding author: e-mail: muhammad.alam@mail.utoronto.ca

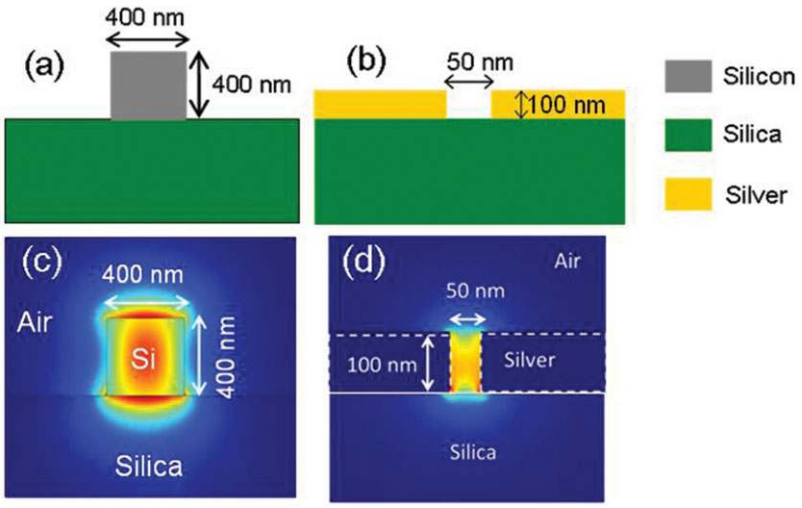

Figure 1 Schematics of (a) SOI waveguide. (b) Metal slot waveguide. (c) and (d) Power confinement of the structures shown in Fig. 1(a) and (b) respectively.

summarizing important progresses in this exciting research area.

The paper is organized as follows. In Sec. 2 we review the principle of operation of the HPWG and discuss some of the HPWGs proposed to date. In Sec. 3 we consider the advantages and limitations of the HPWG. In Sec. 4 we discuss applications of the HPWG for various devices such as polarizers, polarization splitters, polarization rotators, directional couplers, power splitters, microring (microdisk) resonators, modulators, switches, optical tweezers, and nonlinear devices.

Sub-diffraction limited laser is a very important area of HPWG research [11] and has been recently reviewed [12]. Therefore, we would refrain from discussing these devices in detail in this review, and focus mostly on passive devices.

2. Various types of hybrid plasmonic waveguides

The first HPWG was proposed by the researchers at the University of Toronto in 2007 [13]. As shown in Fig. 2(a) the structure consists of a rectangular piece of silicon of dimension 100 nm $\times$ 60 nm separated from a silver surface by a 100 nm thick silica spacer. In the absence of the metal the silicon nanowire supports a dielectric waveguide mode which is concentrated in the silicon core. On the other hand, when silicon nanowire is not present, the metal-silica interface supports a SP mode. When the silicon nanowire is close to the metal surface but separated by a thin spacer layer (e.g. silica), the two modes couple and a super-mode is formed which as shown in Fig. 2(b) is highly concentrated in the low index spacer layer. A detailed analysis of the modes supported by this structure was reported in [14, 15].

It should be pointed out that multilayer waveguides consisting of metal and dielectric layers have been extensively studied in the past; for example in [16], but in a different context. The focus of such works was to use the hybridization of the SP and dielectric waveguide modes to extinguish the TM mode, and design a TE-pass polarizer. The waveguides investigated in [16] had very low index contrast (only a few percent), and as a result the confinement in the spacer region was small. Moreover, there has not been any study on the use of the mode hybridization to implement compact waveguide devices, nor there has been any investigation regarding the possibility of achieving highly localized field intensities using the mode coupling. It is only in recent years and with the introduction of high contrast waveguide platforms such as SOI that it has become possible to design and test HPWGs such as the one shown in Fig. 2.

It should also be pointed out that application of the coupled mode theory in the case of HPWG is not straight forward. Results obtained from conventional coupled mode theory are valid only for large waveguide spacing, i.e. weakly coupling conditions [17]. Non-orthogonal coupled mode theory can provide satisfactory results for strong coupling condition, but only for low index contrast waveguides [18]. In the case of HPWGs, the gap between the two constituent waveguides is usually very small and one of the constituent guides is typically a high index waveguide.

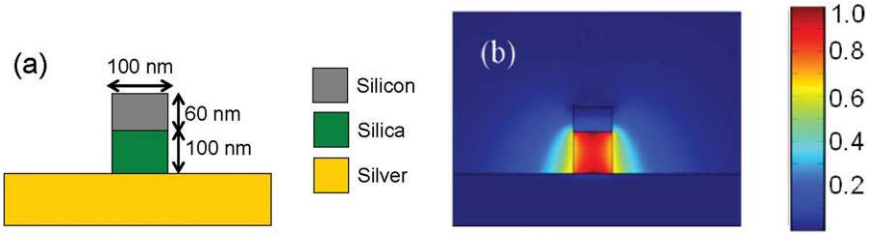

Figure 2 First proposal of the HPWG. (a) Cross section of the structure. (b) Guided power density profile at 0.8 μm wavelength.

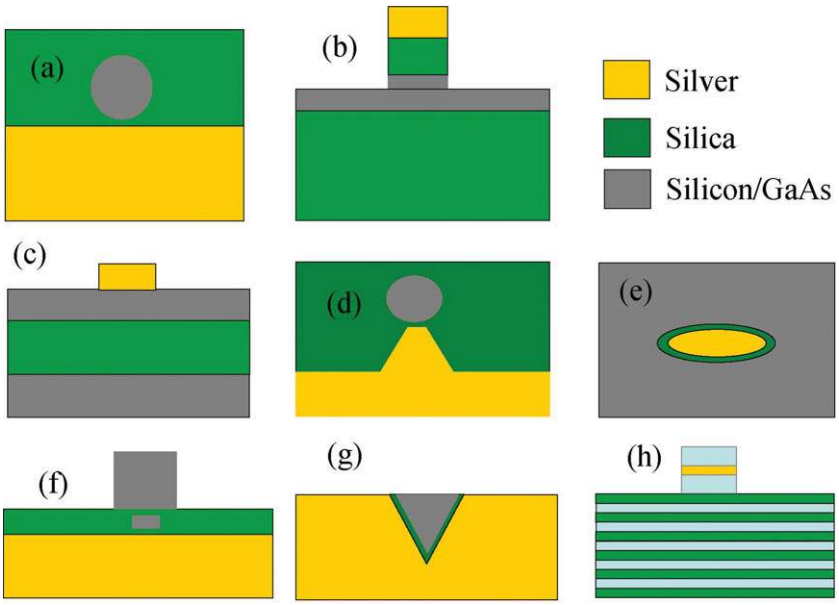

Figure 3 Various types of HPWG.

As a result a straight forward application of the coupled mode theory is not possible. However, this does not mean that coupled modes are not formed in these waveguides. As long as the difference between the effective mode indices of the two constituent waveguide modes is not too large and the guides are in close proximity, coupled modes will be formed. The characteristics of the modes in the HPWGs under various conditions have been studied in [19–25].

Since the first proposal of the HPWG in 2007 [13], many different HPWG structures have been discussed in the literature. Some of these designs are shown in Fig. 3. Figure 3(a) shows the HPWG analyzed by Oulton et al. in 2008 [26]. The structure is very similar to that reported in [13], except for a few minor variations. Instead of the high index silicon waveguide with rectangular cross section considered in [13], Oulton et al. have proposed the use of a high index GaAs waveguide with circular cross section (see also Fig. 2). The structure is difficult to integrate with other components on a chip due to its circular cross section. A comparison between the HPWGs of Refs. [13] and [26] in terms of light confinement will be presented later in this section.

Dai et al. have investigated a HPWG which consists of a metal cap on a SOI ridge guide with a silica spacer (Fig. 3(b)) [27]. A silicon strip loaded with a metal cap with a low index spacer in between was reported in [28]. While the structures reported in [27,28] retain all the advantages of the structures proposed in [13, 26], their implementation is more straightforward. Therefore, many subsequent HPWG devices proposed have used the metal cap topology. Dai et al. have also proposed a HPWG that consists of two nano-slots at the two sides of a high index core [29]. Unlike most other HPWGs which support a TM type hybrid mode, this guide can support a TE hybrid mode. For a 50 nm wide HPWG with double 10 nm wide slots, the power confinement in the nano-slots can be as high as 85%.

Flammer et al. have proposed a HPWG which can be implemented with a combination of surface oxidation and metal patterning (Fig. 3(c)) [30]. Since no etch step is necessary, fabrication of this HPWG is much simpler than most others.

Most HPWGs proposed to date utilizes the coupling of SP supported by a planar metal surface with a dielectric waveguide. The mode size achievable for these guides is limited by the mode size of the SP. Bian et al. have investigated a HPWG consisting of a metal wedge and a high index waveguide (Fig. 3(d)) [31]. Since the mode size of the wedge plasmon is smaller than that of the planar SP, the mode size of the wedge HPWG is also smaller than the planar HPWGs.

Metal nanowires are well known as plasmonic waveguides which have a very high level of light confinement [32]. Kuo et al. have proposed to form a HPWG by separating silicon from a metal nanowire by a silica spacer [33] (Fig. 3(e)). The hybrid mode supported by this guide provides good confinement, long propagation distance, and ease of coupling with dielectric waveguides.

Although in a HPWG the field intensity in the spacer region can be greatly enhanced by reducing the spacer thickness, such an enhancement is accompanied by a reduction in the total power present in the spacer region. In order to simultaneously achieve high field intensity and large field confinement in the spacer, Bian et al. have proposed an HPWG consisting of a high index stripe embedded inside the spacer region between a semiconductor ridge and metal surface [34] (Fig. 3(f)). By combining dielectric slot wave guiding with hybrid plasmonic guiding, this structure can enhance the power confinement by 50% and reduce the mode area by 50 to 60% as compared to conventional HPWG. A combination of channel wave guiding and HPWG was also considered by Bian et al. (Fig. 3(g)) [35]. The waveguide provides significantly better

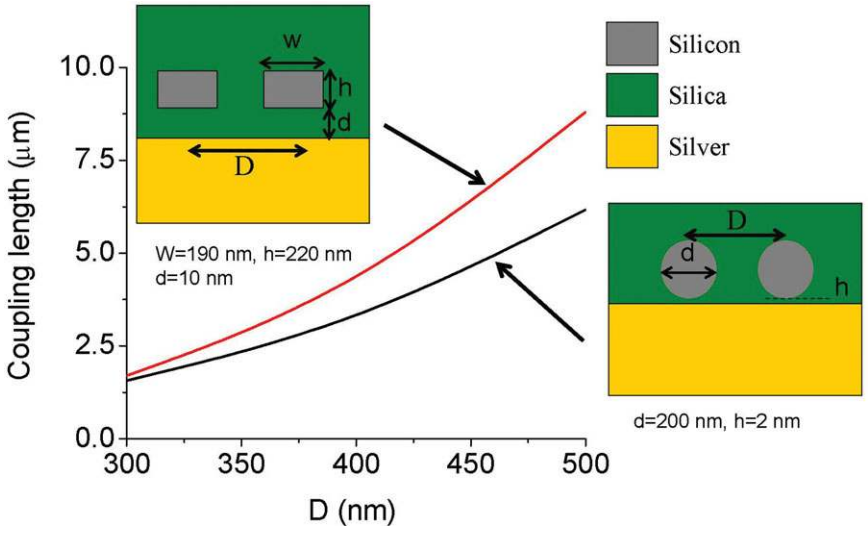

Figure 4 Comparison of coupling lengths for rectangular and circular HPWG for various waveguide spacing (D).

confinement compared to the channel plasmon guides for moderate propagation loss.

Hang et al. have investigated a HPWG consisting of a multilayer dielectric waveguide structure and a metal plane [36] (Fig. 3(h)). Multilayer dielectric waveguides can support surface waves known as Bloch waves, which suffers lower losses than the SP, but their confinement is relatively low. By using the HPWG configuration shown in Fig. 3(h), confinement of the Bloch mode can be greatly enhanced.

The absolute value of the permittivity of a metal is much higher than that of the high index dielectric layer ($|\varepsilon_m| > \varepsilon_{hi}$) in a typical HPWG. Belan et al. analyzed the characteristics of a HPWG when the condition $|\varepsilon_m| < \varepsilon_{hi}$ is satisfied [37]. Their calculation shows that under this condition, a much stronger confinement can be achieved. While the authors have not suggested any particular material system for implementation of this type of HPWG, future work may result in novel devices which utilize this principle.

The above description of various HPWGs is far from complete. Many other types of HPWGs have been investigated numerically and demonstrated experimentally, including symmetric HPWG consisting of a thin metal and two high index layers [38,39], cylindrical HPWG [40], and many others [41–52].

As can be seen from Figs. 2 and 3 both circular and rectangular cross sections of the HPWG have been proposed by various groups. To use the HPWG platform to design practical devices, it is important to know which geometry provides a better performance in terms of the light confinement and losses. A major application area for the HPWG is the integrated optics. For integrated optics, lateral confinement is more important than the vertical confinement. A convenient way of comparing the lateral confinement is to compare the coupling length when two identical HPWG are placed close to each other. In such a comparison, the longer coupling length implies a better light confinement. Figure 4 shows the result of such comparison. According to [26], the minimum mode size for a HPWG with a circular cross section is achieved for a nanowire with 200 nm radius and spacer thickness of 2 nm. A rectangular HPWG with a silicon nanowire width and height of 190 nm and 220 nm and spacer height of 10 nm has the same propagation length as the aforementioned HPWG with circular cross section. Figure 4 compares the coupling lengths as a function of waveguide spacing for these two geometries. From the figure it is evident that the rectangular structure outperforms the circular structure for any waveguide spacing. As a result of various advantages of the rectangular cross section, almost all HPWGs designed and implemented to date use a rectangular cross section.

3. Advantages and limitations of HPWG

Since the HPWG is a combination of a dielectric and a plasmonic waveguide, it provides a number of benefits which are difficult to achieve by either technology alone. The most well known advantage of the HPWG is its ability to offer a better compromise between the loss and confinement than the pure SP mode. This advantage is illustrated in Fig. 5. Figure 5(a) and (b) show the schematics of a HPWG and a single metal-dielectric interface. The dimensions and material properties for the two structures are chosen properly to achieve equal propagation distance for the guided mode for both structures at 1.55 μm wavelength. As the figure indicates the HPWG provides a better compromise between the loss and confinement compared to the purely plasmonic waveguide.

In a conventional dielectric waveguide light is confined in the high index medium. But there are many applications - for example, biosensing and fluorescence - where guiding in a low index medium is preferred. The ability of the HPWG to guide light in the low index medium makes it a very attractive choice for these applications.

Polarization diversity is another distinct advantage of the HPWG over conventional plasmonic waveguides. To illustrate the polarization diversity of the HPWG Fig. 6 shows the mode profiles for both TE and TM modes of a HPWG.

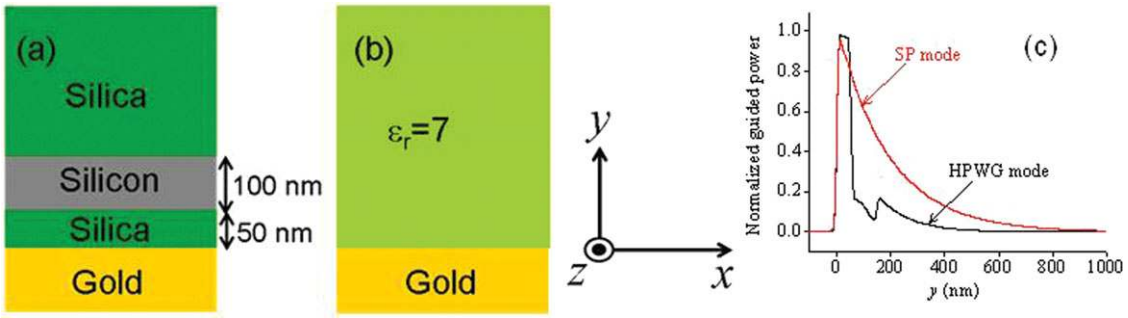

Figure 5 Comparison of guided power density profile for the SP and hybrid modes for the same propagation losses. (a) HPWG waveguide, (b) SP waveguide, (c) guided power density profiles for the two modes at 1.55 μm wavelength. The coordinate system used is also shown. The xz plane coincides with the metal-dielectric interface for both structures. Reproduced from [14].

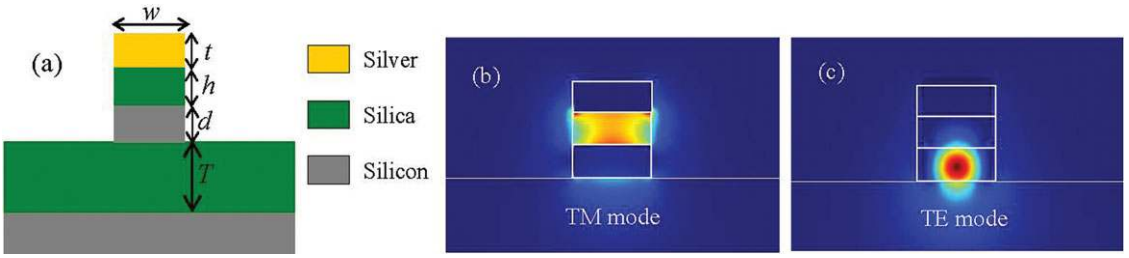

Figure 6 (a) Schematic of the HPWG cross section. (b) Power density profile for the TM mode in the cross section. (c) Power density profile for the TE mode in the cross section. Wavelength of operation is 1.55 μm. Dimensions of the waveguide are $w = 350$ nm, $t = 200$ nm, $h = 150$ nm, $d = 150$ nm and T = 2 μm.

The structure supports a TM mode, which is of a hybrid nature, and concentrated in the low index spacer region as shown in Fig. 6(b). The TE mode, on the other hand, is concentrated in the high index layer as shown in Fig. 6(c). Since the TE and TM modes are guided in two different regions, their behavior can be adjusted almost independent of each other by changing the properties and dimensions of the corresponding layers. This diversity in polarization, as compared to conventional plasmonic waveguides which only support TM modes, can be utilized to design devices where the control of polarization is important. Some examples of such devices are: polarizers, polarization rotators, and new types of sensors and biosensors.

The large propagation loss of the plasmonic guides makes the implementation of fully plasmonic circuits impractical for most applications. A more realistic approach would be to integrate plasmonic devices with other high index contrast waveguides - for example, waveguides based on the SOI platform. In such cases, the dielectric waveguides can guide the light into and out of the plasmonic or HPWGs, and the plasmonics or HPWGs can be used to execute a specific function - for example, polarization control, modulation, or sensing. Fabrication of HPWGs is fully compatible with the standard fabrication processes used in integrated optics, and HPWGs offer the opportunity to simultaneously take advantages of both SOI and plasmonics technologies.

Despite their many advantages, HPWGs have also some limitations which should be carefully considered. Although HPWGs provide a better compromise between loss and confinement as compared to purely plasmonic guides, they still suffer large propagation losses as compared to purely dielectric waveguides. Some of the claims regarding the superiority of the HPWGs over other plasmonic guides are in our judgment too strong. This confusion arises from the difficulty in choosing a proper definition of the mode size for plasmonic guides. Unlike dielectric waveguides whose field profiles are usually circular or elliptical, the field profiles of plasmonic guides are more complicated, and there is no general agreement on how the mode size of various plasmonic guides should be compared. Oulton et al. in their well-known work on HPWG [26], defined the mode size as

$$A = \frac{1}{\max\{W(r)\}} \int W(r) dA \qquad (1)$$

Here, $W(r)$ is the energy density of the mode at location r and the two dimensional integration is carried out up to infinity over the cross section of the waveguide. Using this definition they concluded that the mode size for the HPWG is at least an order of magnitude smaller (for comparable propagation distance) than previously reported plasmonic guides. Although HPWGs provide very high field intensity and good confinement, a significant amount of power is still concentrated in the high index nanowire. Therefore, this definition of mode size is not an indication of the true extent of the guided mode or the overall mode profile. Among

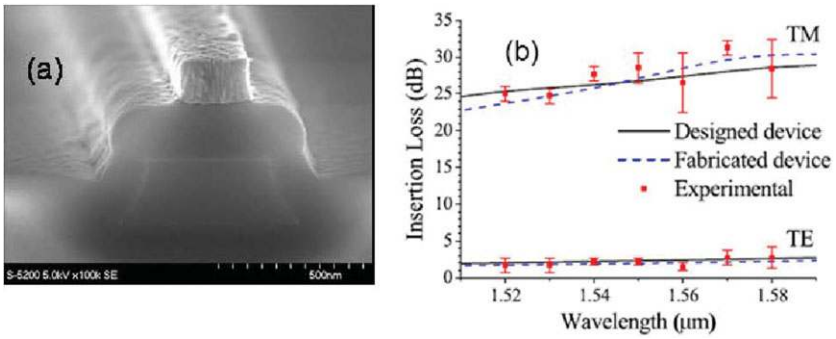

Figure 7 (a) SEM image of the HPWG TE-pass polarizer (b) Insertion loss for TE and TM modes for a 30 μm long HPWG TE-pass polarizer. Reproduced from [57].

the plasmonic researchers, this definition of the mode size has been used only by the HPWG researchers. Results of the comparison of plasmonic waveguides can be different depending on the definition of the mode size used. The issue has been discussed in detail in [53–55].

Another limitation of HPWGs is the fabrication complexity required to produce these devices. Unlike dielectric waveguides, which can be fabricated by a single etch step, fabrication of HPWG requires more steps. This fact should also be taken into account when considering the cost of using HPWG for a particular application.

4. Applications of HPWG

As explained in Sec. 3, HPWG offers number of important advantages, for example, compatibility with silicon photonics, good compromise between loss and confinement, polarization diversity and ability to guide light in low index medium. Not surprisingly, there has been a major effort to utilize these properties for various applications. Here we briefly review some of the major application areas of HPWG.

4.1. Passive integrated optic devices

4.1.1. Polarization control devices

The on-chip control of polarization is very important for ensuring proper operation of many photonic devices, especially in the case of high index contrast systems such as SOI. The concept of HPWG can be used to implement various polarization control devices such as TE- and TM-pass polarizers, polarization rotators and polarization splitters.

The design of a HPWG based TE-pass polarizer was reported in [56]. This device uses the fact that since the TM mode is confined in the spacer close to the metal, it is always more lossy than the TE mode. By choosing the material properties and waveguide dimensions properly, it is possible to make the propagation loss of the TM mode to be much larger than that of the TE mode [56]. Sun et al. have experimentally demonstrated a TE-pass polarizer using the same principle as shown in Fig. 7(a) [57]. This is the shortest broadband SOI based TE-pass polarizer reported to date [58]. As shown in Fig. 7(b), insertion losses for both TE and TM modes match very well with simulation results for their design.

When the spacer of the HPWG is relatively thick (on the order of hundred nanometers or more) the TE mode in HPWG is relatively unaffected by the presence of metal. However the situation changes significantly for a thin spacer layer. Although noble metals such as gold and silver cannot be considered to be perfect conductors at optical wavelengths, they still can be considered "good conductors" i.e., their permittivities have large negative real parts and as a result they oppose the existence of tangential electric field on the surface. As a result, for a thin spacer layer, the TE mode which has the dominant electric field tangential to the metal surface is pushed out of the core and reaches cut off. A design of a TM-pass polarizer was presented in [59] which utilizes this property. The simulated extinction ratio and insertion loss for the TM-mode are 21.8 dB and 3.2 dB, respectively.

Chee et al. have experimentally demonstrated a HPWG polarization splitter (Fig. 8(a)) [60]. The central part of the device is a three-way coupler shown in Fig. 8(b), which consist of a Cu-SiO_2-Si HPWG sandwiched between two silicon waveguides. The dimensions of the HPWG are chosen in such a way that it supports only the TM mode. As the result a TM mode launched at the input waveguide transfers from one silicon waveguide to the other silicon waveguide through the HPWG, while no such coupling takes places for the TE mode (it stays in the input waveguide). Figure 8(c) shows the normalized transmission of both modes for a 6.4 μm long splitter. Extinction ratios of 12.3 and 13.9 dB were achieved for the TE and TM modes, together with insertion losses of 2.8 dB and 6 dB, respectively.

L. Gao et al. proposed an alternate design of HPWG based polarization splitter [61]. Their device is an asymmetric directional coupler consisting of a HPWG separated from a silicon waveguide by a small gap. The large asymmetry of the directional coupler results in high birefringence. As a result, TM modes supported by the two guides couple strongly; whereas, the coupling for the TE mode is weak. For 4.13 μm device length, they predicted extinction ratios of 20.9 dB and 16.4 dB for the TM and TE modes, respectively.

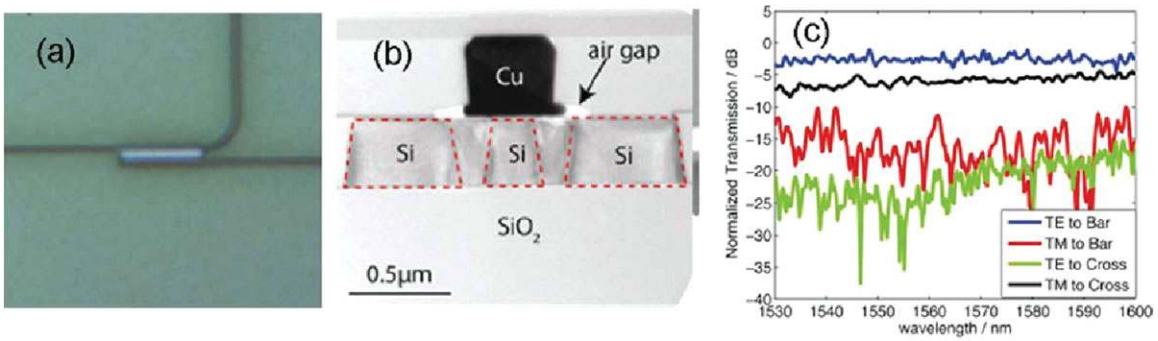

Figure 8 (a) Optical microscope image of the HPWG polarization splitter (b) Cross section of the HPWG (c) Transmission spectra. Reproduced from [60].

Polarization rotator is another very important component for on chip control of polarization. Most polarization rotator designs reported to date are based on either mode interference or adiabatic mode evolution. The former is compact (∼10 μm) but have narrow bandwidth (∼25 nm) [62]. The latter, on the hand, require longer length (>100 μm) to achieve sufficient extinction ratio and they usually require uncommonly thick silicon waveguides or additional material layers [63, 64]. Caspers et al. have proposed [65] and experimentally demonstrated [66] a HPWG polarization rotator. The device consists of a silicon waveguide separated from a silver film by a thin silica spacer layer (Fig. 9(a)). The width of the silicon and thickness of the spacer is kept constant but the width of the silver film gradually decreases along the length of the device. The electric field tends to stay orthogonal to the metal surface. Therefore, as the silver is tapered away from the top of the metal, the input TM mode of the waveguide is converted into a TE mode. An SEM image of a fabricated polarization rotator is shown in Fig. 9(b) and the performance of the device for various device lengths is shown in Fig. 9(c). For a 3.7 μm long device, the device provides a polarization extinction ratio of 13.5 dB, while the insertion loss for the device can be as low as 1.5 dB.

4.1.2. Directional couplers and power splitters

Power dividers and couplers are among the most common components in integrated optics. Various compact HPWG power dividers and couplers with good performance characteristics have been proposed.

Dai et al. have proposed a compact 50:50 multimode interference (MMI) power splitter using the HPWG [67]. The length and width of the MMI section are 500 nm and 650 nm, respectively; and 500 nm long tapers at both input and output are used. The predicted power transmission of the coupler is more is about 91%. Various design issues for HPWG power splitter, and Mach-Zehnder interferometer have been analyzed in Refs. [68, 69].

HPWG directional couplers have been investigated by many researchers [68–75]. These devices can be used to overcome some of the limitations of dielectric waveguide directional couplers. Examples of such limitations are: coupler's narrow-band response and sensitivity to the excitation wavelength.

The power transfer efficiency of a directional coupler depends on the ratio of the field amplitudes and their relative phases at the inputs. This dependency can be used to make a cascade of directional couplers where the overall system is wavelength insensitive. By tuning the length of the first coupler and the length of the phase delay line, one can control the input field amplitude and phase for the second coupler in such a way that it cancels out the wavelength dependency of the first coupler section. A design to achieve a broadband coupler operation based on this principle, where a HPWG is used to implement a phase delay line, was reported in [70]. The device consists of two symmetric silicon waveguide couplers connected by an asymmetric section which

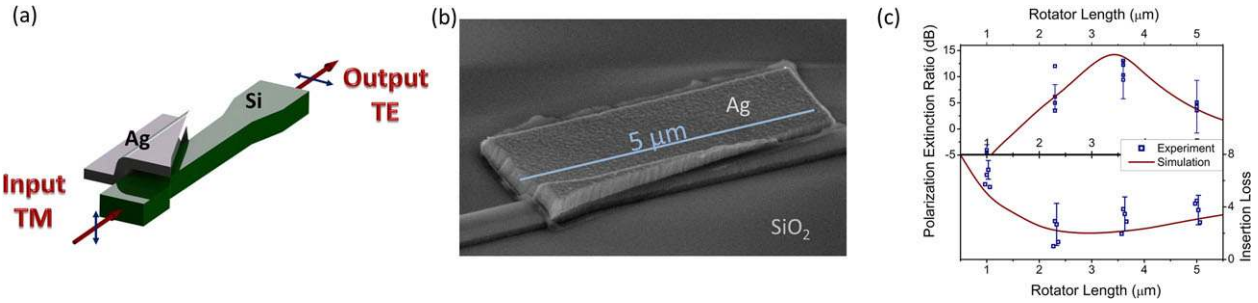

Figure 9 (a) Schematic of the polarization rotator (b) SEM image of the fabricated device (c) Extinction ratio and insertion loss of the rotator for various device lengths. Reproduced from [66].

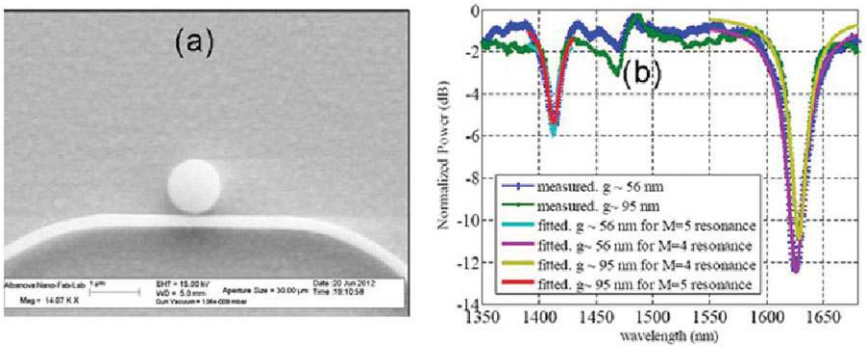

Figure 10 (a) SEM image of HPWG microdisk resonator. (b) Transmission spectra. Reproduced from [76].

consists of a silicon waveguide separated from a HPWG. By adjusting the lengths of the two symmetric coupler sections and by adjusting the phase delay provided by the asymmetric section, broadband operation over 150 nm for a coupler length of only 8.3 μm can be achieved.

Another limitation of directional couplers is their high polarization dependency. This is especially true for high index contrast SOI waveguides. For a given polarization (TE or TM) the coupling length of a directional coupler corresponding to that polarization (L_C^i, i = TE or TM) is given by $L_C^i = \pi/\Delta\beta^i$, where $\Delta\beta^i$ is the phase difference between the even and odd TE or TM supermodes. Since in a HPWG the TE and TM modes are confined in two different layers, the properties of these two modes can be controlled independently in such a way that $\Delta\beta^i$ becomes equal for both polarizations for the same length. The device then operates as a polarization independent coupler [71].

Lou et al. have experimentally demonstrated an ultra-compact HPWG directional coupler [72]. The measured coupling length for their device was as small as 1.55 μm, and propagation loss of the HPWG was 0.08 dB/μm which makes it a good candidate for future ultra-dense photonics integrated circuits (PICs).

4.1.3. Microring and microdisk resonators

Microring and microdisk resonators are useful for many applications including filtering, optical modulation and biosensing. HPWG based microring and microdisk resonators have been numerically and experimentally investigated by a number of groups [76–84]. Lou et al. have fabricated microdisk resonators consisting of a 56 nm thick layer of silica sandwiched between a gold layer and 400 nm thick amorphous silicon layer (Fig. 10(a)) [76]. Transmission spectra for some of their fabricated devices are shown in Fig. 10(b). The extinction ratio for the 5th and 4th order resonances of a microdisk resonator of 525 nm radius are 5.5 dB and 10 dB, respectively; and the quality factor for these two resonances are 350 and 110, respectively.

Tang et al. have investigated microring resonators for which the metal is horizontally separated from the high index medium [77] to reduce the radiation losses. FDTD simulation predicts an extinction ratio of 13 dB and a free spectral range of 260 nm for a microring radius of 0.5 μm.

Silicon has a large positive thermo-optic coefficient. As a result, microring resonators based on silicon waveguides or gold-silica-silicon HPWG are highly sensitive to temperature, which may limit their use in many applications. Zhu et al. proposed the idea of replacing the silica spacer with a material with negative thermo-optic coefficient (e.g. titanium oxide, TiO_2) to achieve athermal operation [78]. They chose copper, instead of gold, as a metal to make the HPWG more compatible with CMOS fabrication technology (Fig. 11). For a Cu-TiO_2-Si HPWG microring resonator they experimentally demonstrated a 50% reduction in thermal sensitivity as compared to a Cu-SiO_2-Si device.

High index contrast HPWG (e.g. those using silicon and CdS) although compact in size, also has larger propagation loss. Horvath et al. suggested the use of lower index contrast

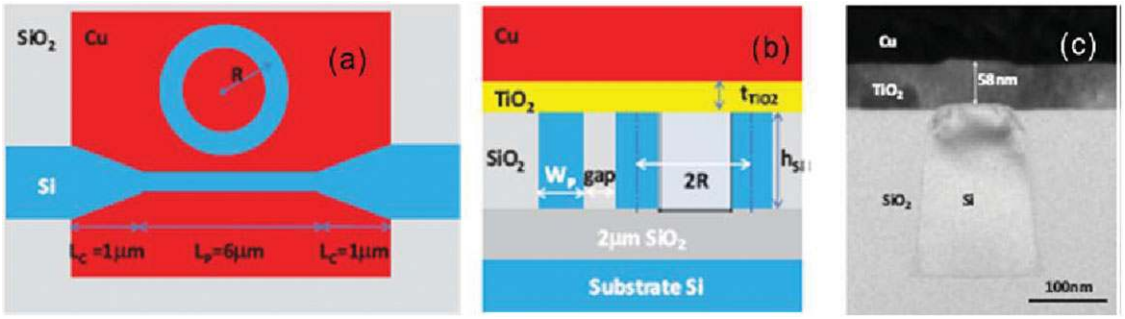

Figure 11 (a) Schematic of a Cu-TiO_2-Si HPWG ring resonator (b) Cross section of the waveguide. (c) XTEM image of the fabricated HPWG. Reproduced from [78].

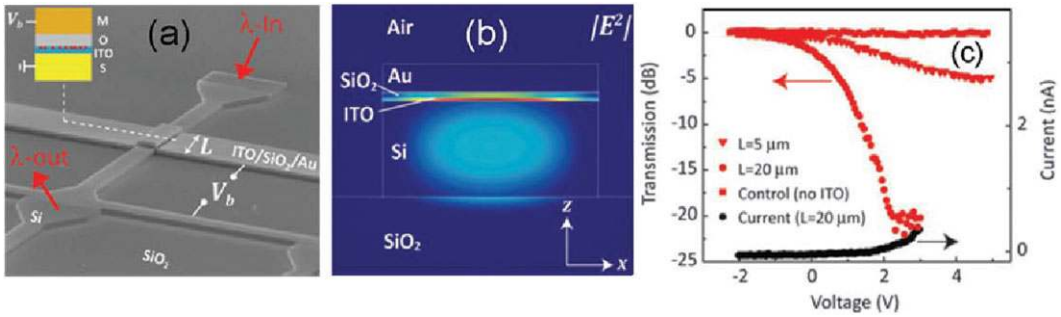

Figure 12 (a) SEM image of HPWG electrooptic modulator (b) Electric field intensity in the active region of modulator (c) Modulator performance for various drive voltage. Reproduced from [86].

HPWG to reduce the loss [79]. By using a Au/Silica/SU-8 HPWG, they achieved quality factor close to 300, which is among the highest for plasmonic microring resonators.

Since microring and microdisk resonators require waveguide bends, radiation loss becomes an issue for small band radius. To minimize radiation loss and crosstalk between adjacent waveguide, the HPWG structure proposed in [85] can be considered. In this case the metal is separated from the high index medium by a horizontal gap, which reduces the cross talk between adjacent HPWG devices.

4.2. Modulators and switches

Electro-optic modulators and switches are among the most important components for optical communication. Silicon based electro-optic modulators usually depend on weak nonlinear effects and are large in size. Microring resonators can reduce the modulator size but they have a narrow bandwidth and are highly sensitive to temperature. A number of HPWG modulators and switches have been proposed to overcome the above limitations [86–90].

Sorger et al. have experimentally demonstrated a modulator using a gold-ITO-silicon HPWG [86] (Fig. 12(a)). When a forward bias voltage (gold is positive and silicon is grounded) is applied across the waveguide, an accumulation layer is formed inside the HPWG which increases the imaginary part of the refractive index of the ITO and hence the propagation loss of the HPWG increases. Figure 12(a) shows the fabricated device. As shown in Fig. 12(b) the electric field density for the active region of the device is highly concentrated in the ITO layer. The extinction ratio for 5 μm and 20 μm long devices was reported to be 5 dB and more than 20 dB, respectively. The transmission characteristics of the device are shown in Fig. 12(c). The high extinction ratio, moderate insertion loss and large bandwidth (more than 1000 nm) makes the device a very attractive candidate for future PICs.

Mott insulators (e.g. vanadium oxide) experience a metal/insulator phase transition under thermal or electrical excitations. Such a transition results in a large change in material properties. For example the index of VO_2 changes from $n = 3.243+0.3466i$ for the insulating phase to $n = 1.977+2.53i$ in the metallic phase at a wavelength of 1550 nm. Joushaghani et al. demonstrated a sub-volt hybrid plasmonic VO_2 switch (Fig. 13(a)) [87]. The device is formed by depositing a 300 nm thick silver film on a 820 nm silica spacer layer over a VO_2 film. A 5 μm wide strip perpendicular to the waveguide acts as a thin film heater to heat the local volume of VO_2. The mode profiles for two different temperatures are shown in Fig. 13(b) and (c). This change in mode profiles is accompanied by a large change in propagation losses. Figure 13(d) shows the measured transmission as a function of input current. The switching bandwidth of the device exceeds 100 nm and 400 mV drive voltage is sufficient to achieve an extinction ratio over 20 dB.

Ooi et al. have proposed using a metal-TiO_2-VO_2-TiO_2-metal waveguide to implement a compact electro absorption modulator [88]. When the VO_2 is in metallic phase, the device acts like a metal-insulator-metal waveguide and light passing through the guide experiences large attenuation.

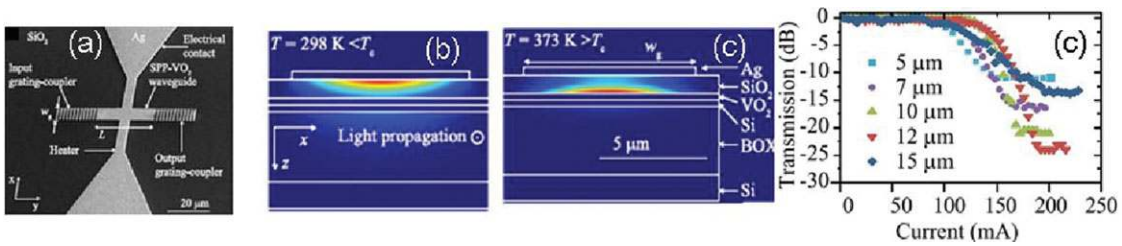

Figure 13 (a) SEM image of VO_2 broadband coupler (b) and (c) Electric field intensities of the guided modes for two different temperatures. (d) Transmission of the device for various input currents. Reproduced from [87].

The device in this situation is in the off-state. When the VO_2 turns to the insulator phase, the waveguide acts like a HPWG and power is confined in the low loss TiO_2 spacer layer. The propagation loss of the guided mode is thus greatly reduced and the device is in the on-state. According to the numerical calculations presented in [88] a 200 nm long modulator can provide a modulation depth of around 10 dB and low insertion loss (∼1 dB). The predicted driving voltage for the device is 4.6V and the total energy consumption is only 2.6 fJ/bit.

Sun et al. have proposed a modulator that consists of a Ag-Polymer-Si-Polymer-Ag structure [89]. Since the structure has two spacer layers on two sides of the silicon core, it supports two hybrid modes having different field profiles and effective mode indices. As these two modes propagate down the HPWG, power transfers from one waveguide to the other periodically, which affects the power coupled to the output waveguide. According to their finite element simulation when no voltage is applied to the modulator the power transmission through the device is 16% and it drops to 1% when 6 volt voltage is applied across the HPWG, i.e., the device can provide an extinction ratio of 12 dB at 6 volt driving voltage. The device has a very small capacitance and parasitic resistance, and as a result it has a modulation bandwidth of more than 40 GHz. Power consumption predicted at this speed is 0.27 mW.

Finally, Li et al. have investigated the design of a 16-point quadrature amplitude modulation scheme using the HPWG [90]. The design uses two HPWG based phase shifters where highly nonlinear polymer is used as the spacer medium. They predict that for a device size of less than 100 μm, a modulation bandwidth of more than 1 THz can be achieved with an insertion loss of approximately 5.17 dB.

4.3. Optical force and optical tweezers

The optical force for a waveguide mode can be obtained from the dispersion relation [91]

$$F = \frac{n_g}{n_{eff}c}\left.\frac{\partial n_{eff}}{\partial g}\right|_k PL \tag{2}$$

Here n_g and n_{eff} are the group index and effective index of the guided mode, g is the spacing between the two waveguides which will be the spacer region height in case of HPWG, c is the speed of light, L is the length of the waveguide, k is the wave vector, and $U = n_g PL/c$ is the total energy stored in the optical mode. The formation of HPWG results in strong energy localization in the spacer region, and as a result, HPWG can exhibit optical forces which are orders of magnitude higher than these guides, as has been theoretically predicted by Yang et al. [91], and analyzed further in [92, 93]. H. Li et al. has recently measured the magnitude of optical forces in the HPWGs [92]. They implemented a HPWG which is formed by separating a free standing section of silicon waveguide from a metal by a small air gap. By using a Mach-Zehnder interferometer they verified the existence of significant optical forces in the HPWG. For a gap size of 20 nm, the measured optical force per unit length was approximately 100 pN/μm.mW, which is 200 times larger than that of a silicon nanowire coupled to a silica substrate. Because of its small size and large optical force, HPWG can be very useful for various applications including reconfigurable optical circuits, mechanical memory operation, and all optical signal processing.

Due to the diffraction limited size of optical beams, it is very difficult to manipulate nano size objects using conventional optical traps. As pointed by Yang et al. it is very difficult to trap nanoparticles of size less than 14 nm with 1.5 watt optical power for a single beam gradient optical trap [91]. Optical trapping force on a nanoparticle is given by

$$F = -\frac{n_m}{2}\alpha\nabla E^2 \tag{3}$$

Here, n_m is the refractive index of the medium surrounding the particle, α is the polarizability of the particle and E^2 is the square of the magnitude of the electric field. The large energy concentration in the spacer layer of the HPWG and the large field gradient in this region make the HPWG very attractive for optical trapping application. Yang et al. have carried out a theoretical investigation of the possibility of using the HPWG for optical trapping [91]. According to their calculation, for a polystyrene particle of 5 nm diameter, the optical force in a HPWG with a circular cross section of the high index medium, the optical trapping force can be 435 fN/W whereas the force is only 11.6 fN/W in the photonic mode. In addition, as one crosses the center point along the horizontal direction, the sign of the force is reversed, which indicates that a nanoparticle should be trapped exactly underneath the waveguide. This phenomenon can be used to implement optical tweezers for various nanoscale applications.

4.4. Nonlinear devices

Plasmonic waveguides have a number of features which are very beneficial for nonlinear effects. Using a plasmonic guide, one can achieve very high field intensity on the metal surface which will enhance nonlinear effects significantly. In addition the properties of plasmonic modes are also highly sensitive to the dielectric properties near the metal surface. Thus it is possible to use a control beam to modify the properties of a material on the metal surface, which in turn controls the propagation of a signal beam Additionally the response of plasmonic signal can be on the order of few femtoseconds which offers the possibility of ultrafast signal processing. Because of these advantages nonlinear plasmonics has been a very active area of research [94]. Many promising applications of nonlinear plasmonics are ultimately limited by the large loss of plasmonic modes. Since HPWG offers a combination of low loss and high power density, it has attracted a lot of attention for various nonlinear applications, including second harmonic

generation, parametric amplification and phase regeneration of optical signals [95–101].

Y. Su has analyzed a step-structure HPWG for application in nonlinear optics [95]. The structure is similar to the one proposed by Dai et al. [27], with the exception that in addition to a metal cap above the high index ridge, it also has a metal cladding which extends on both sides. With these extra degrees of freedom, this structure can attain a good compromise between loss and confinement. The optimized structure can confine light to a mode area of $(\lambda/180)^2$ and a propagation distance of 172 is μm. By filling the gap spacer region by the highly nonlinear polymer region regular poly 3-Hexy 1 Thiophene (RR-P3HT), the achieved nonlinearity can be 2 to 3 orders larger than that of conventional silicon waveguide. For a 0.5 watt input power, this structure acts as a parametric oscillator with a peak gain of 14 dB and the 3 dB gain bandwidth covers the entire C, L and S bands.

Lu et al. have investigated the second harmonic generation efficiency of a HPWG consisting of a Lithium Niobate slab separated from a silver film by a small air gap [96]. The air gap here plays the dual role of reducing propagation loss and increasing field confinement, which enhances nonlinear interactions. The fundamental mode of this structure (1.55 μm wavelength) is a hybrid mode and concentrated in both high index medium (Lithium Niobate) and air gap. Power for the second harmonic (775 nm) is concentrated in the high index layer. For 1 watt input power, the second harmonic generation efficiency can be around 1.3% and the maximum of second harmonic is reached over a distance of 1 mm in this case. Although the overlap between the fundamental and second harmonic modes are slightly less than those of purely plasmonic guides, the reduced loss of the HPWG greatly increases the second harmonic generation efficiency in the former case. The second harmonic generation efficiency of the HPWG described in Lu. et al. is on the order of a few percentage whereas that of a dielectric loaded SP guide is only 0.024%.

J. Zhang et al. have investigated the phase relation between the signal and pump wave in a symmetric HPWG [97]. Their numerical analysis showed that when the phase of the incoming signal wave is around π but not differing by more than $\pi/2$, it stabilizes to π after propagating through HPWG in presence of the pump wave. If on the other hand, the phase of the signal wave is around zero but not different by more than $\pi/2$, then it stabilizes to zero. They proposed to use this phase squeezing phenomenon to regeneration of phase shift keyed (PSK) signal. The use of HPWG for phase regeneration has two advantages: It can regenerate phase over a very short distance (less than 200 μm) and the characteristics of the phase regenerator can be tuned by controlling the phase of the pump wave. Such a device can be very useful for all-optical signal processing in future nanophotonic circuits.

4.5. Biosensor

The energy of surface plasmon waves is highly concentrated at a metal/dielectric interface and as a result such waves are very sensitive to any change near the metal surface. Since the hybrid mode provides a higher concentration of power near the metal surface as compared to surface plasmons [14], it also offers a higher sensitivity to changes on the surface [102–106]. Zhou et al. investigated a HPWG sensor based on the microring configuration [102]. The predicted sensitivity of their device is 580 nm/RIU which is much larger than those of dielectric waveguide resonator (163 nm/RIU) and dielectric slot waveguide (298 nm/RIU). The radius of the HPWG microring resonator is also much smaller (1 μm) as compared to the slot waveguide (5 μm). Such a sensor can be very useful for lab-on-chip biosensing system.

Although plasmonics has established itself as the dominant technology for affinity biosensing, it suffers from a number of limitations. Since a conventional plasmonic sensor only supports a TM mode, the number of linearly independent measurements that such a sensor can carry out is limited. For example, for conventional plasmonic sensor, it is very difficult (if not impossible) to determine both adlayer index and adlayer thickness and one of these two is usually assumed known. It is also difficult to differentiate between the bulk and surface changes and such separation requires an additional reference channel. Since the HPWG supports both TE and TM modes, the number of independent measurements it can provide is twice the conventional plasmonic sensors. As a result a HPWG sensor can be used to simultaneously detect the adlayer thickness and index. Furthermore, to separate the bulk and surface changes a HPWG sensor does not require a reference channel (i.e. it can perform a self-referenced measurement) [103, 104].

4.6. Gain medium and laser

Although losses associated with the HPWG are lower than many plasmonic guides, further reduction of losses will make the HPWG more attractive for many applications. One way to reduce the propagation losses (or even make the waveguide lossless) is to incorporate a gain medium in the HPWG [107–110]. Depending on the geometry and material properties, the gain required for lossless propagation can be greatly different. Dai et al. have investigated the gain requirement for a HPWG consisting of an inverted top metal rib separated from a high index rib structure [107]. According to their calculation, the loss can be completely compensated when using a low index medium with gain 176 dB/cm. If the high index region is the gain medium, the gain required is about 200 dB/cm. Zhang et al. have investigated a HPWG consisting of a silver cladding layer with a semi-cylindrical bump on top of an InGaAsP nanowire. The gain required for lossless propagation in this case is approximately 1223 cm^{-1} [108]. Gain required for lossless propagation in a HPWG similar to the one described in [30] was investigated by L. Gao et al. [109]. In this case, power confinement is relatively low, and as a result gain requirement for lossless propagation is also lower (3.8 cm^{-1}). Very recently almost 100% loss compensation

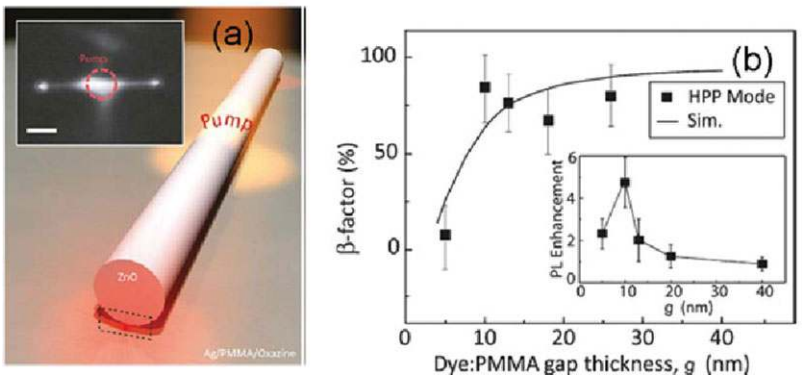

Figure 14 (a) Schematic of the HPWG formed by dye doped PMMA sandwiched between a silver film and ZnO nanowire. Photoluminescence (PL) image in the inset shows emission from dye molecules excited at the center of the waveguide (marked by dashed circle) coupling to deep subwavelength mode and scattering to far field at the ends of the waveguide. (b) Variation of spontaneous emission (β) and PL enhancement with gap thickness (g). Reproduced from [112].

for a CdSe nanobelt/Al_2O_3/Ag guide was experimentally demonstrated [110].

4.7. Other applications

Although the previous subsections summarizes some of the major areas of HPWG research, the list is far from complete. For example, Luo et al. have designed an on-chip HPWG light concentrator [111]. Using a taper of submicron length on a gold-silica-silicon nitride structure, they achieved a field concentration factor of above 13.

The high level of localization of light achievable in the HPWG makes it very attractive for fluorescence enhancement as has been experimentally demonstrated by Sorger et al. In their experiment they fabricated a ZnO semiconductor nanowire on a PMMA coated silver surface [112]. The PMMA contained oxazine dye molecules and as a result the dye molecules in the spacer region experience the high field intensity resulting from formation of the hybrid mode [Fig. [14](a)]. Sorger et al. have measured a reduction in emission life time up to 60 times relative to the intrinsic lifetime of dye molecules over the spectral bandwidth of emission. About 85% of the molecular emission couples to the HPWG mode, and the photoluminescence is enhanced by five times (Fig. 14(b)) [112]. Such a structure is promising for applications in transfer of quantum information and efficient light extraction beyond cavity limited bandwidth. Efficient coupling of dielectric and HPWG waveguides is important for most applications. A number of works to achieve this have been reported [113–117].

5. Perspective and challenges

Although hybrid plasmonics is a relatively new area of research, the activity in this field has been truly impressive. Many devices including polarizers, modulators, couplers, lasers, light concentrator, nonlinear devices and biosensors have been proposed and experimentally demonstrated. However, other areas where the HPWG can find useful applications remain relatively unexplored. Most HPWG devices are designed for silicon on insulator platform. Although there has been some theoretical investigation of HPWGs on other semiconductors such as AlGaAs and InP, there is a scarcity of experimental work in this area. More work in this area may result in useful and novel devices; for example, compact and highly efficient nonlinear devices.

The concept of HPWG can also be used to implement very compact devices at longer wavelengths. Since at longer wavelengths, there are more choices for materials with high index of refraction, there is potential for new types of devices at these wavelengths.

Another relatively less studied area is sensors and biosensors based on the HPWG platform. The high intensity optical fields achieved by HPWGs can be used to make novel and more sensitive sensors. For example, metal nanoparticles can be placed in the spacer region of a HPWG to improve the sensitivity of Raman spectroscopy.

Finally, as it is the case with any practical field, when designing a new device it is important to carefully consider the limitations of the technology being used. It is also important to choose the proper figure of merit when comparing the performances of devices designed for different purposes.

Received: 7 October 2013, **Revised:** 7 December 2013, **Accepted:** 12 December 2013

Published online: 24 February 2014

Key words: surface plasmon, plasmonics, hybrid plasmonic waveguide, integrated optics.

Muhammad Zulfiker Alam received his Ph.D. from the University of Toronto in 2012, his M A. Sc. from the University of Victoria in 2004, and his B. Sc. Engineering from Bangladesh University of Engineering and Technology in 2000. For his Ph.D. research work he received the Douglas R. Colton Medal for Research Excellence, which is given to one researcher every year in Canada in recognition of excellence in research leading to new understanding and novel developments in microsystems and related technologies. He is currently a post-doctoral fellow in the Photonics group of the University of Toronto. His research interests include plasmonics, integrated optics and optical sensing.

J. Stewart Aitchison received the B.Sc. and Ph.D. degrees from The Physics Department, Heriot-Watt University, Edinburgh, Scotland, U.K., in 1984 and 1987, respectively. His dissertation work was on optical bistability in semiconductor waveguides. From 1988 to 1990, he was a post-doctoral Member of Technical Staff with Bellcore, NJ., where his research interests were in the areas of highly nonlinear glasses and spatial soliton propagation. He joined The Department of Electronics and Electrical Engineering at The University of Glasgow, Glasgow, Scotland, U.K., in 1990 as a Lecturer and was promoted to Professor of Photonics in 1999. His research focused on nonlinear optics, planar silica and optical biosensors. In 1996, he was the holder of a Royal Society of Edinburgh Personal Fellowship to carry out research on spatial solitons at CREOL, the College of Optics and Photonics at the University of Central Florida. Since 2001 he has held the Nortel Chair in Emerging Technology in the Department of Electrical and Computer Engineering at the University of Toronto. Dr. Aitchison is a fellow of the Institute of Physics, the Optical Society of America, the American Association for the Advancement of Science (AAAS) and the Royal Society of Canada.

Mo Mojahedi received his Ph.D. from the University of New Mexico (UNM), Center for High Technology Materials (CHTM), in December 1999 (with distinction). For his Ph.D. work he received the Popejoy award which is the highest honor given every three years to the most outstanding Ph.D. dissertation across Engineering, Physics, and Chemistry at UNM. From February 2000 to June 2001 he worked as a Research Assistant Professor at CHTM in collaboration with the Department of Physics at the University of California at Berkeley. In 2001 he joined the Department of Electrical and Computer Engineering at the University of Toronto. From September 2007 to January 2010 Prof. Mojahedi was the director of the University of Toronto's Emerging Communications Technology Institute (ECTI) – an interdisciplinary Open Research Facility dedicated to micro- and nano-technology and fabrication. Professor Mojahedi's scientific interests include novel macro and nanoscale photonic and microwave devices, plasmonics, optical sensors, wave matter interaction, and fundamental electromagnetic theory.

References

[1] W. L. Barnes, A. Dereux, and T. W. Ebbesen, Nature **424**, 824–830 (2003).
[2] J. Homola, Anal Bional Chem **377**(3), 528–539 (2003).
[3] E. Ozbay, Science **311**(5758), 189–193 (2006).
[4] G. Veronis and S. Fan, J. of Light. Tech. **25**(9), 2511–2521 (2007).
[5] J. A. Dionne, L. A. Sweatlock, and H. A. Atwater, Phys. Rev. B **73**, 035407 (2006).
[6] L. Liu, Z. Han, and S. He, Opt. Exp. **13**(17), 6645–6650 (2005).
[7] P. Berini, (OSA) Advances in Opt. and Photon. **1**, 484–588 (2009).
[8] S. I. Bozhevolnyi, V. S. Volkov, E. Devaux, J.-Y. Laluet, and T. W. Ebbesen, Nature **440**, 508–511 (2006).
[9] B. Steinberger, A. Hohenau, H. Ditlbacher, A. L. Stepanov, and A. Dretz, Appl. Phys. Lett. **88**, 094104 (2006).
[10] D. F. P. Pile, T. Ogawa, D. K. Gramotnev, T. Okamoto, M. Haraguchi, M. Fukui, and S. Matsuo, Appl. Phys. Lett. **87**, 061106 (2005).
[11] R. F. Oulton, V. J. Sorger, T. Zentgraf, R.M. Ma, C. Gladden, L. Dai, G. Bartal, and X. Zhang, Nature **461**, 629–632 (2009).
[12] R.-M. Ma, R. F. Oulton, V. J. Sorger, and X. Zhang, Lasers and Photonics Rev. **7**(1), 1–21 (2013).
[13] M. Z. Alam, J. Meier, J. S. Aitchison, and M. Mojahedi, "Super mode propagation in low index medium", http://www.opticsinfobase.org/abstract.cfm?uri=CLEO-2007-JThD112, CLEO/QELS 2007.
[14] M. Z. Alam, J. Meier, J. S. Aitchison, and M. Mojahedi, Opt. Exp. **18**(12), 12971–12979 (2010).
[15] M. Z. Alam, Hybrid plasmonic waveguides: Theory and applications, PhD Thesis, (University of Toronto, 2012).
[16] C. Rashleigh, Opt. and Quantum Electron. **8**(1), 49–60 (1976).
[17] A. Hardy, and W. Streifer, J. Lightwave Tech. **3**(5), 1135–1146 (1985).
[18] A. W. Snyder, A. Ankiewicz, and A. Atlintas, Electron. Lett. **23**(20), 1097–1098 (1987).
[19] M. Z. Alam, J. S. Aitchison, and M. Mojahedi, IEEE J. of Sel. Topics in Quantum Electron. **19**(3), 4602008 (2013).
[20] M. Fujii, J. Leuthold, and W. Freude, IEEE Photon. Tech. Lett. **21**(6), 362–364 (2009).
[21] L. Zhu, IEEE Photon. Tech. Lett. **22**(8), 535–537 (2010).
[22] Y. Bian and Q. Gong, Opt. Comm. **308**(1), 30–35 (2013).
[23] P.-J. Cheng, C.-Y. Weng, S.-W. Chang, T.-R. Lin, and C.-H. Tien, IEEE J. of Sel. Topics in Quantum Electron. **19**(3), 4800306 (2013).
[24] R. Zeng, Y. Zhang, and S. He, Front. Optoelectron. **5**(1), 68–72 (2012).
[25] T. Sharma and V. Mehta, Int. J. of Adv. Res. Comp. Commun. Eng. **2**(5), 2135–2137 (2013).
[26] R. F. Oulton, V. J. Sorger, D. A. Genov, D. F. P. Pile, and X. Zhang, Nature Photon. **2**, 496–500 (2008).
[27] D. Dai and S. He, Opt. Exp. **17**(19), 16646–16653 (2009).
[28] M. Wu, Z. Han, and V. Van, Opt. Exp. **18**(11), 11728–11736 (2010).
[29] D. Dai and S. He, Opt. Exp. **18**(17), 17958–17966 (2010).
[30] P. D. Flammer, J. M. Banks, T. E. Furtak, C. G. Durfee, R. E. Hollingsworth, and R. T. Collins, Opt. Exp. **18**(20), 21013–21023 (2010).
[31] Y. Bian, Z. Zheng, Y. Liu, J. Liu, J. Zhu, and T. Zhou, Opt. Exp. **19**(23), 22417–22422 (2011).
[32] J. Takahara, S. Yamagishi, H. Taki, A. Morimoto, and T. Kobayashi, Op. Lett. **22**(7), 475–477 (1997).
[33] Y. Kou, F. Ye, and X. Chen, Opt. Exp. **19**(12), 11746–11752 (2011).

[34] Y. Bian, Z. Zheng, X. Zhao, L. Liu, Y. Su, J. Liu, J. Zhu, and T. Zhou, J. Opt. **15**(3), 035503 (2013).
[35] Y. Bian, Z. Zheng, X Zhao, L. Liu, Y. Su, J. Liu, J. Zhu, and T. Zhou, J. Opt. **15**(5), 055011 (2013).
[36] W. Y. Hang, Z. Zheng, S. X. Gang, B. Y. Sheng, and L. J. Sheng, Science China Tech. Sci. **56**(3), 567–572 (2013).
[37] S. Belan, S. Vergeles, and P. Vorolov, Opt. Exp. **21**(6), 7427–7438 (2013).
[38] Y. Bian, Z. Zheng, X. Zhao, J. Zhu, and T. Zhou, Opt. Exp. **17**(23), 21320–21325 (2009).
[39] L. Chen, T. Zhang, X. Li, and W. Huang, Opt. Exp. **20**(18), 20535–20544 (2012).
[40] D. Chen, Appl. Opt. **49**(36), 6868–6871 (2010).
[41] Q. Huang, F. Bao, and S. He, Opt. Exp. **21**(2), 1430–1439 (2013).
[42] I. Goykhman, B. Desiatov, and U. Levy, Appl. Phys. Lett. **97**, 141106 (2010).
[43] C.-C. Huang, IEEE J. of Sel. Topics in Quant. Electron. **18**(6), 1661–1668 (2012).
[44] C.-L. Zou, F.-W. Sun, C.-H. Dong, Y.-F. Xiao, X.-F. Ren, L. Kv, X.-D. Chen, J. Cui, Z.-F. Han, and G.-C. Guo, IEEE Photon. Tech. Lett. **24**(6), 434–436 (2012).
[45] L. Chen, X. Li, G. Wang, W. Li, S. Chen, L. Xiao, and D. Gao, J. Lightwave Tech. **30**(1), 163–168 (2012).
[46] Q. Lu, F.-J. Shu, and C. L. Zou, http://arxiv.org/abs/1310.2318 (2013).
[47] Y. Ma, G. Farrell, Y. Semenova, H. P. Chan, H. Zhang and Q. Wu, Plasmonics **8**(2), 1259–1263 (2013).
[48] Shruti, R. K. Sinha, and R. Bhattacharyya, J. Opt. Soc. Am. A **30**(8), 1502–1507 (2013).
[49] M.-S. Kwon, Opt. Exp. **19**(9), 8379–8393 (2011).
[50] M.-S. Kwon, J.-S. Shin, S.-Y. Shin, and W.-G. Lee, Opt. Exp. **20**(20), 21875–21887 (2012).
[51] A. Amirhosseini and R. Safian, IEEE Transactions on Nanotechnology **12**(6), 1031–1036 (2013).
[52] X. Zuo and Z. Sun, Opt. Lett. **36**(15), 2946–2948 (2011).
[53] R. F. Oulton, G. Bartal, D. F. Pile, and X. Zhang, New J. Physics **10**, 105018 (2008).
[54] R. Buckley and P. Berini, Opt. Exp. **15**(19), 12174–12182, (2007).
[55] X. Sun, M. Z. Alam, J. S. Aitchison, and M. Mojahedi, IEEE Photonics Conference 618–619 (2012).
[56] M. Z. Alam, J. S. Aitchison, and M. Mojahedi, Opt. Lett. **37**(1), 55–57 (2012).
[57] X. Sun, M. Z. Alam, S. J. Wagner, J. S. Aitchison, and M. Mojahedi, Opt. Lett. **37**, 4814–4816 (2012).
[58] I. Avrutsky, IEEE J. of Selected Topics in Quantum Electron. **14**(6), 1509–1514, (2008).
[59] M. Z. Alam, J. S. Aitchison, and M. Mojahedi, Appl. Opt. **50**(15), 2294–2298 (2011).
[60] J. Chee, S. Zhu, and G. Q. Lo, Opt. Exp. **20**(23), 25345–25355 (2012).
[61] L. Gao, F. Hu, X. Wang, L. Tang, and Z. Zhou, Appl. Phys. B **113**(2), 199–203 (2013).
[62] A. V. Velasco, M. L. Calvo, P. Cheben, A. Ortega-Moñux, J. H. Schmid, C. A. Ramos, Í. M. Fernandez, J. Lapointe, M. Vachon, S. Janz, and D.-X. Xu, Opt. Lett. **37**(3), 365–367 (2012).
[63] J. Zhang, M. Yu, G.-Q. Lo, and D.-L. Kwong, IEEE J. Sel. Top. Quantum Electron. **16**(1), 53–60 (2010).
[64] L. Chen, C. R. Doerr, and Y.-K. Chen, Opt. Lett. **36**(4), 469–471 (2011).
[65] J. N. Caspers, M. Z. Alam, and M. Mojahedi, Opt. Lett. **37**(22), 4615–4617 (2012).
[66] J. N. Caspers, J. S. Aitchison, and M. Mojahedi, Opt. Lett. **38**(20), 4054–4057 (2013).
[67] J. Wang, X. Guan, Y. He, Y. Shi, Z. Wang, S. He, P. Holmström, L. Wosinski, L. Thylen, and D. Dai, Opt. Exp. **19**(2), 838–847 (2011)
[68] J. Ctyroký, P. Kwiecien, and I. Richter, J. of the European Optical Society – Rapid Publications **8**, 13024 (2013).
[69] X.-Y. Zhang, A. Hu, J. Z. Wen, T. Zhang, X.-J. Xue, Y. Zhou, and W. W. Duley, Opt. Exp. **18**(18), 18945–18959 (2010).
[70] M. Z. Alam, J. N. Caspers, J. S. Aitchison, and M. Mojahedi, Opt. Exp. **21**(13), 16029–16034 (2013).
[71] M. Z. Alam, J. S. Aitchison, and M. Mojahedi, Opt. Lett. **37**(16), 3417–3419 (2012).
[72] F. Lou, Z. Wang, D. Dai, L. Thylen, and L. Wosinski, Appl. Phys. Lett. **100**, 241105 (2012).
[73] H.-S. Chu, E.-P. Li, and R. Hegde, Appl. Phys. Lett. **96**, 221103 (2010).
[74] Q. Li, Y. Song, G. Zhou, Y. Su, and M. Qiu, Opt. Lett. **35**(19), 3153–3155 (2010).
[75] M. T. Noghani and M. H. V. Samiei, Appl. Opt. **52**(31), 7498–7503 (2013).
[76] F. Lou, L. Thylen, and L. Wosinski, Proc. SPIE **8781**, 87810X (2013).
[77] L. Tang, F. Hu, H. Yi, and Z. Zhou, Proc. SPIE **8564**, 856417 (2012).
[78] S. Zhu, G.-Q. Lo, L. Xie, and D.-L. Kwong, IEEE Photon. Tech. Lett. **25**(12), 1161–1164 (2013).
[79] C. Horvath, D. Bachman, M. Wu, D. Perron, and V. Van, IEEE Photon. Tech. Lett. **23**(17), 1267–1269 (2011).
[80] H.-S. Chu, Y. Akimov, P. Bai, and E.-P. Li, Opt. Lett. **37**(21), 4564–4566 (2012).
[81] S. Zhu, G. Q. Lo, and D. L. Kwong, Opt. Exp. **20**(14), 15232–15246 (2012).
[82] D. Dai and S. He, Proc. SPIE **8265**, 82650L (2012).
[83] H.-S. Chu, Y. A. Akimov, P. Bai, and E.-P. Li, J. Opt. Soc. Am. B **28**(12), 2895–2901 (2011).
[84] S. Zhu, G.-Q Lo, and D.-L. Kwong, IEEE Photon. Tech. Lett. **24**(14), 1224–1226 (2012).
[85] Y. Song, M. Yan, Q. Yang, L. Tong, and M. Qiu, Opt. Comm. **284**(1), 480–484 (2011).
[86] V. J. Sorger, N. D. L-Kimura, R.-M. Ma, and X. Zhang, Nanophotonics **1**(1), 17–22 (2012).
[87] A. Joushaghani, B. A. Kruger, S. Paradis, D. Alain, J. S. Aitchison, and J. K. S. Poon, Appl. Phys. Lett. **102**, 061101 (2013).
[88] K. J. A. Ooi, P. Bai, H. S. Chu, and L. K. Ang, Nanophotonics **2**(1), 13–19 (2013).
[89] X. Sun, L. Zhou, X. Li, Z Hong, and J. Chen, Appl. Opt. **50**(20), 3428–3434 (2011).
[90] F. Li, M. Xu, X. Hu, J. Wu, T. Wang, and Y. Su, Opt. Comm. **286**, 166–170 (2013).
[91] X. Yang, Y. Liu, R. F. Oulton, X. Yin, and X. Zhang, Nano Lett. **11**(2), 321–328 (2011).
[92] H. Li, W. Noh, Y. Chen, and M. Li, Opt. Exp. **21**(10), 11839–11851 (2013).

[93] Z. Lu and Y. Shu, Chin. Phys. Lett. **30**(3), 034208 (2013).
[94] M. Kauranen and A. V. Zayats, Nature Photon. **6**, 737–748 (2012).
[95] Y. Su, Asia Communications and Photonics Conference, 732–734 (2010).
[96] F. F. Lu, T. Li, X. P. Hu, Q. Q. Cheng, S. N. Zhu, and Y. Y. Zhu, Opt. Lett. **36**(17), 3371–3373 (2011).
[97] J. Zhang, P. Zhao, E. Cassan, and X. Zhang, Opt. Lett. **38**(6), 848–850 (2013).
[98] S. Aldawsari, Nonlinear hybrid plasmonic waveguides, M.Sc. Thesis (University of Waterloo, 2013).
[99] A. Pitilakis, O. Tsilipakos, and E. Kriezis, ICTON, paper: Mo. C5.5 (2012).
[100] K.-Y. Wang and A. C. Foster, Integrated Photonics Research, Silicon and Nanophotonics, OSA Tech. Digest, paper JTuB15 (2011).
[101] Z. Zhang, J. Wang, C. Xinag, and C. Gui, Asia Communications and Photonics Conference, OSA Tech. Digest, paper: AF4A.14 (2012).
[102] L. Zhou, X. Sun, X. Li, and J. Chen, Sensors **11**(7), 6856–6867 (2011).
[103] F. Bahrami, M. Z. Alam, J. S. Aitchison, and M. Mojahedi, Plasmonics **8**(2), 465–473 (2013).
[104] M. Z. Alam, F. Bahrami, J. S. Aitchison, and M. Mojahedi, Submitted to IEEE Photon. Journal.
[105] Y. Q. Ma, G. Farrell, Y. Semenova, and Q. Wu, Proc. SPIE **8812**, 88120T (2013).
[106] M. S. Kwon, Plasmonics **5**(4), 347–354 (2010).
[107] D. Dai, Y. Shi, S. He, L. Wosinski, and L. Thylen, Opt. Exp. **19**(14), 12925–12936 (2011).
[108] J. Zhang, L. Cai, W. Bai, Xu, and G. Song, Opt. Lett. **36**(12), 2312–2314 (2011).
[109] L. Gao, L. Tang, F. Hu, R. Guo, X. Wang, and Z. Zhou, Opt. Exp. **20**(10), 11487–11495 (2012).
[110] N. Liu, H. Wie, J. Li, Z. Wang, X. Tian, A. Pan, and H. Xu, Scientific Reports 3: 1967 (2013).
[111] Y. Luo, M. Chamanzer, and A. Abidi, Opt. Exp. **21**(2), 1898–1910 (2013).
[112] V. J. Sorger, N. Pholchai, E. Cubukcu, R. F. Oulton, P. Kolchin, C. Borschel, M. Gnauck, C. Ronning, and X. Zhang, Nano. Lett. **11**(11), 4907–4911 (2011).
[113] P. Shi, G. Zhou, and F. S. Chau, J. Opt. Soc. Am. B **30**(6), 1426–1431 (2013).
[114] L. Chen, X. Li, and D. Gao, Appl. Phys. B **111**(1), 15–19 (2013).
[115] V. D. Ta, R. Chen, and H. D. Sun, Opt. Exp. **19**(14), 13598–13603 (2011).
[116] Y. Song, J. Wang, Q. Li, M. Yan, and M. Qiu, Opt. Exp. **18**(12), 13173–13179 (2010).
[117] Y. Song, J. Wang, M. Yan, and M. Qiu, J. Opt. **13**(7), 075002 (2011).